

Intravoxel water diffusion heterogeneity MR imaging of nasopharyngeal carcinoma using stretched exponential diffusion model

Vincent Lai · Victor Ho Fun Lee · Ka On Lam · Henry Chun Kin Sze · Queenie Chan · Pek Lan Khong

Received: 24 July 2014 / Revised: 28 September 2014 / Accepted: 20 November 2014 / Published online: 23 December 2014
© European Society of Radiology 2014

Abstract

Purpose To determine the utility of stretched exponential diffusion model in characterisation of the water diffusion heterogeneity in different tumour stages of nasopharyngeal carcinoma (NPC).

Materials and methods Fifty patients with newly diagnosed NPC were prospectively recruited. Diffusion-weighted MR imaging was performed using five b values (0–2,500 s/mm²). Respective stretched exponential parameters (DDC, distributed diffusion coefficient; and alpha (α), water heterogeneity) were calculated. Patients were stratified into low and high tumour stage groups based on the American Joint Committee on Cancer (AJCC) staging for determination of the

predictive powers of DDC and α using t test and ROC curve analyses.

Results The mean±standard deviation values were DDC=0.692±0.199 ($\times 10^{-3}$ mm²/s) for low stage group vs 0.794±0.253 ($\times 10^{-3}$ mm²/s) for high stage group; α =0.792±0.145 for low stage group vs 0.698±0.155 for high stage group. α was significantly lower in the high stage group while DDC was negatively correlated. DDC and α were both reliable independent predictors ($p<0.001$), with α being more powerful. Optimal cut-off values were (sensitivity, specificity, positive likelihood ratio, negative likelihood ratio) DDC=0.692 $\times 10^{-3}$ mm²/s (94.4 %, 64.3 %, 2.64, 0.09), α =0.720 (72.2 %, 100 %, –, 0.28).

Conclusion The heterogeneity index α is robust and can potentially help in staging and grading prediction in NPC.

Key Points

- Stretched exponential diffusion models can help in tissue characterisation in nasopharyngeal carcinoma
- α and distributed diffusion coefficient (DDC) are negatively correlated
- α is a robust heterogeneity index marker
- α can potentially help in staging and grading prediction

V. Lai (✉) · P. L. Khong

Department of Diagnostic Radiology, Li Ka Shing Faculty of Medicine, Queen Mary Hospital, University of Hong Kong, Room 406, Block K, Pok Fu Lam, Hong Kong
e-mail: vincentlai166@yahoo.com.hk

P. L. Khong

e-mail: plkhong@hku.hk

V. H. F. Lee · K. O. Lam · H. C. K. Sze

Department of Clinical Oncology, Li Ka Shing Faculty of Medicine, Queen Mary Hospital, University of Hong Kong, 1/F Professorial Block, Pok Fu Lam, Hong Kong

V. H. F. Lee

e-mail: vhflee@hku.hk

K. O. Lam

e-mail: lamkaon@hku.hk

H. C. K. Sze

e-mail: hcksze@hku.hk

Q. Chan

Philips Healthcare, Hong Kong, 6/F, Core Building 1, 1 Science Park East Avenue, Hong Kong Science Park, Shatin, New Territories, Hong Kong
e-mail: queenie.chan@philips.com

Keywords Nasopharyngeal carcinoma ·

Diffusion weighted imaging · Magnetic resonance imaging · Stretched exponential · Staging

Abbreviations

α	Alpha (intravoxel water diffusion heterogeneity)
AJCC	American Joint Committee on Cancer
AUC	Area under curve
DDC	Distributed diffusion coefficient
DW	Diffusion-weighted
F-	18-fluoro-2-deoxyglucose
FDG	
IVIM	Intravoxel incoherent motion

MR	Magnetic resonance
NPC	Nasopharyngeal carcinoma
PET/CT	Positron emission tomography with computed tomography
ROC	Receiver operating characteristic
ROI	Region-of-interest
SD	Standard deviation
SNR	Signal-to-noise ratio
SPIR	Spectral presaturation inversion recovery
STIR	Short TI inversion recovery
TFE	Turbo-field-echo
TR/TE	Repetition time/echo time
TSE	Turbo spin echo

Introduction

Nasopharyngeal carcinoma (NPC) is endemic in Southeast Asia. Accurate staging is imperative for optimal treatment planning. Conventional magnetic resonance (MR) imaging has excellent diagnostic accuracy in the depiction and delineation of the tumour, but with lack of functional information. We then commonly rely on 18-fluoro-2-deoxy-glucose (^{18}F -FDG) positron emission tomography with computed tomography (PET/CT) imaging but with the risk of radiation exposure. Diffusion-weighted (DW) MR imaging has been shown to be useful in the functional evaluation of NPC, allowing a noninvasive means of tumour characterisation [1]. In particular, the intravoxel incoherent motion (IVIM) biexponential diffusion model is one type of DW MR imaging which has shown promising results in tissue characterisation and treatment monitoring studies [2–4]. The IVIM biexponential model is advantageous over the conventional monoexponential model in that it allows separation of pure diffusion and perfusion properties, and provides their estimates [5]. While pure diffusion had been shown to be a reliable predictor with high reproducibility, the reliability and reproducibility of the perfusion estimates have been a major concern [6].

The stretched exponential diffusion model is an alternative model to characterise the diffusion signal in a multicompartiment model using the Kohlrausch decay function [7–9]. It provides a measure of signal deviation from the monoexponential behaviour caused by pseudoperfusion effects, hence giving information on diffusion and intravoxel heterogeneity. It was thought to be a more suitable model for diffusion-weighted signal decay due to the heterogeneous environment of the spins [10]. In addition, the parameters derived had been shown to be more reliable and reproducible [11]. However, this type of diffusion model has yet to be properly tested in NPC so far.

In this study, we aimed to determine the potential utility of the stretched exponential diffusion model in the characterisation of the diffusion heterogeneity in different tumour stages of NPC, hence its ability in the prediction of tumour staging and prognostication.

Materials and methods

Patient selection

A prospective study was carried out after institutional review board approval with written informed consent was obtained. Patients with newly diagnosed biopsy-proven NPC seen in our institution from May 2013 to March 2014 were consecutively recruited. The main inclusion criterion was patients with first episode of newly diagnosed histologically proven NPC. Major exclusion criteria included (a) prior treatment of any form given already; (b) concurrent head and neck diseases or other tumours.

A total of 53 patients with newly diagnosed histologically proven undifferentiated NPC were initially recruited. Other histological subtypes of NPC were not identified in our cohort. Three patients were later excluded because of small tumour volumes ($<30.00\text{ mm}^3$) or motion artefacts with resultant reduced signal-to-noise ratio (SNR) in region-of-interest (ROI) analysis of DW images. Therefore, a total of 50 patients (40 male, 10 female; mean age 53.04 ± 12.61 years, range 26–83 years) were subsequently included. American Joint Committee on Cancer (AJCC) and TNM stages for all patients were then devised by three independent clinical oncologists subspecialized in NPC, based on available clinical and imaging findings (MR imaging of the nasopharynx and neck, computed tomography scan of the thorax and abdomen or whole body ^{18}F -FDG PET/CT). Any discrepancy was resolved after subsequent consensus. The clinical demographic data and distribution of the AJCC and TNM stages of all patients are listed in Table 1.

Conventional MR imaging techniques

All MR imaging was performed with a 3.0-T MR scanner (Achieva 3.0T, Philips Healthcare, Best, the Netherlands), utilizing a 16-channel neurovascular coil. Four standard sequences were performed: (a) axial T1-weighted turbo spin echo (TSE) [repetition time/echo time (TR/TE), 454/9.2 ms; turbo factor, 3; FOV, 230×230 mm; matrix, 672×672 ; slice number, 32; slice thickness, 3 mm; intersection gap, 0.3 mm]; (b) axial T2-weighted short TI inversion recovery (STIR) [TR/TE, 4,644/60 ms; FOV, 230×230 mm; matrix, 672×672 ; slice number, 32; slice thickness, 3 mm; intersection gap, 0.3 mm]; (c) coronal T2-weighted STIR [TR/TE, 4,644/60 ms; FOV, 230×230 mm; matrix, 480×480 ; slice number, 32; slice

Table 1 Clinical and demographic data for all patients

N	50
Sex	
Male	40
Female	10
Age (years)	53.04±12.61 (26–83)
Tumour volume (mm ³)	1,334.29±1,978.01 (53.2–10,098.60)
AJCC staging	
I	5 (10 %)
II	9 (18 %)
III	25 (50 %)
IV	11 (22 %)
T staging	
T1	21 (42 %)
T2	5 (10 %)
T3	15 (30 %)
T4	9 (18 %)
N staging	
N0	10 (20 %)
N1	13 (26 %)
N2	24 (48 %)
N3	3 (6 %)
M staging	
M0	48 (96 %)
M1	2 (4 %)

AJCC American Joint Committee on Cancer

thickness, 3 mm; intersection gap, 0.3 mm]; (d) 3D T1-weighted turbo-field-echo (TFE) post-contrast scan [TR/TE, 4.8/2.4 ms; flip angle, 10°; FOV, 230×230 mm; matrix, 640×640; slice number, 319; slice thickness, 0.72 mm]. Intravenous bolus injection of gadopentetate dimeglumine (0.1 mmol/kg body weight) was administered at 1.5 mL/s for post-contrast acquisition after the DW MR sequence was performed.

Diffusion-weighted MR imaging

DW MR imaging was performed utilizing a single-shot spin-echo echo-planar imaging sequence, with the following parameters: TR/TE, 7,996/43 ms; echo-planar imaging factor, 35; sensitivity encoding factor, 3.5; FOV, 230×230 mm; slice thickness, 3 mm; intersection gap, 0.3 mm; matrix, 256×256; receiver bandwidth, 2,735.7 Hz/pixel; motion probing gradients in three orthogonal axes; number of signal averages, 3; parallel imaging (SENSitivity Encoding [SENSE]) factor, 3; spectral presaturation inversion recovery (SPIR) fat suppression. Image acquisition was performed in the axial plane covering the nasopharynx, with 18 slices obtained. A total of

five b values were used: 0, 500, 1,000, 2,000 and 2,500 s/mm². The scanning time was about 7 min.

Image and data analysis

Individual DW images for the three directions were automatically averaged, and the averaged DW images were then included for subsequent analysis. The stretched exponential model was introduced by Bennett et al. [7, 8] and described by the following formula:

$$S(b)/S_0 = \exp[-(b \times \text{DDC})^\alpha]$$

where $S(b)$ is the signal magnitude with diffusion weighting b , S_0 is the signal magnitude with no diffusion weighting, b is the b value, α is the intravoxel water diffusion heterogeneity (ranging between 0 and 1) and DDC is the distributed diffusion coefficient reflecting the mean intravoxel diffusion rate. α is a relatively new parameter and corresponds to the heterogeneity index. When $\alpha=1$, it points towards low intravoxel diffusion heterogeneity; when $\alpha=0$, it signifies high intravoxel diffusion heterogeneity related to multiexponential decay.

All image analysis were performed on in-house software developed in IDL 6.3 (ITT Visual Information Solutions, Boulder, CO) and fitted on a pixel-by-pixel basis using a nonlinear least-squares routine to create isotropic α and DDC maps [7–9]. Matlab (The MathWorks, Natick, Massachusetts) was used to label voxels with low SNR as “not-a-number” and they were removed from subsequent analysis. Only pixels with signals safely above background noises were included for calculation.

An ROI was manually drawn by a radiologist (specialized in head and neck radiology) to contour the border of NPC on each slice in order to obtain the total tumour volume. The total tumour volume was then calculated on the basis of the segmentation method. Each ROI was contoured on STIR T2W images (Fig. 1a) and co-registered to DW images (Fig. 1b) for analysis using Image J (NIH, Bethesda, MD). Each lesion was measured twice in two separate sessions at 2 weeks apart to ensure reproducibility. The obtained parameters for each lesion were then calculated on a pixel-by-pixel basis and expressed as means of the whole volume analysed.

Statistical analysis

Patients were stratified into two groups for statistical analysis by combining AJCC stage I and II ($n=14$) into a low stage group, and AJCC stage III and IV ($n=36$) into a high stage group. This was because of the small patient numbers in stage I ($n=5$) and stage II ($n=9$) diseases.

Univariate analysis using Student's t test was carried out to compare α and DDC between the low and high stage groups. Box-whisker plots were obtained to illustrate the group-wise

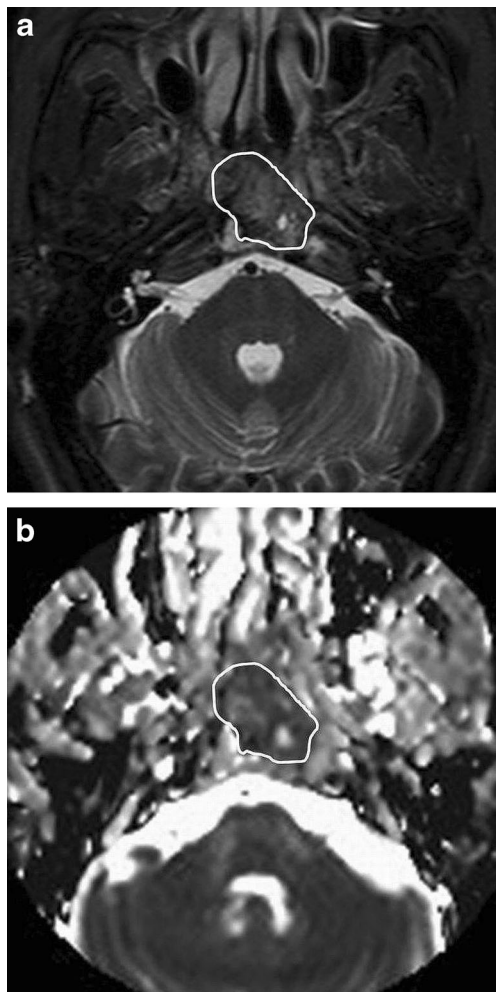


Fig. 1 **a** A 46-year-old man with stage T3 nasopharyngeal carcinoma (NPC). Axial T2-weighted STIR image showing region of interest (ROI) contouring the margin of NPC. **b** Co-registration of the ROI onto the corresponding axial diffusion-weighted image

differences. Receiver operating characteristic (ROC) curves were generated with respective cut-off values determined to accommodate the best diagnostic accuracy based on the Youden index. All statistical analyses were performed by SPSS version 21 for windows. A *p* value of less than 0.05 was considered statistically significant.

Results

The intraobserver agreement was good with a kappa value (κ) for α and DDC of 0.81 and 0.77 respectively. The mean tumour volume was $1,334.29 \pm 1,978.01 \text{ mm}^3$ (53.2–10,098.60). The mean values of α and DDC in the low and high stage groups for AJCC staging are summarized in Table 2 and represented in respective box plots (Fig. 2a and b). Their respective optimal cut-off values upon ROC curve analyses are summarized in Table 3 and shown in Fig. 3.

Table 2 Mean values of the distributed diffusion coefficient (DDC) and diffusion heterogeneity (α) with respective *p* values between low stage and high stage groups for AJCC staging according to Student's *t* test analysis

AJCC stage	<i>n</i> (50)	DDC ($\times 10^{-3} \text{ mm}^2/\text{s}$)	Alpha (α)
Low (I+II)	14	0.692 ± 0.199	0.792 ± 0.145
High (III+IV)	36	0.794 ± 0.253	0.698 ± 0.155
<i>p</i> value		$p < 0.001$	$p < 0.001$

AJCC American Joint Committee on Cancer

DDC was statistically significantly higher in the high stage group while α was statistically lower in the high stage group as compared with the low stage group. The mean \pm standard deviation (SD) values were as follows: DDC = 0.692 ± 0.199 ($\times 10^{-3} \text{ mm}^2/\text{s}$) for the low stage group vs 0.794 ± 0.253 ($\times 10^{-3} \text{ mm}^2/\text{s}$) for high stage group ($p < 0.001$); $\alpha = 0.792 \pm 0.145$ for the low stage group vs 0.698 ± 0.155 for the high

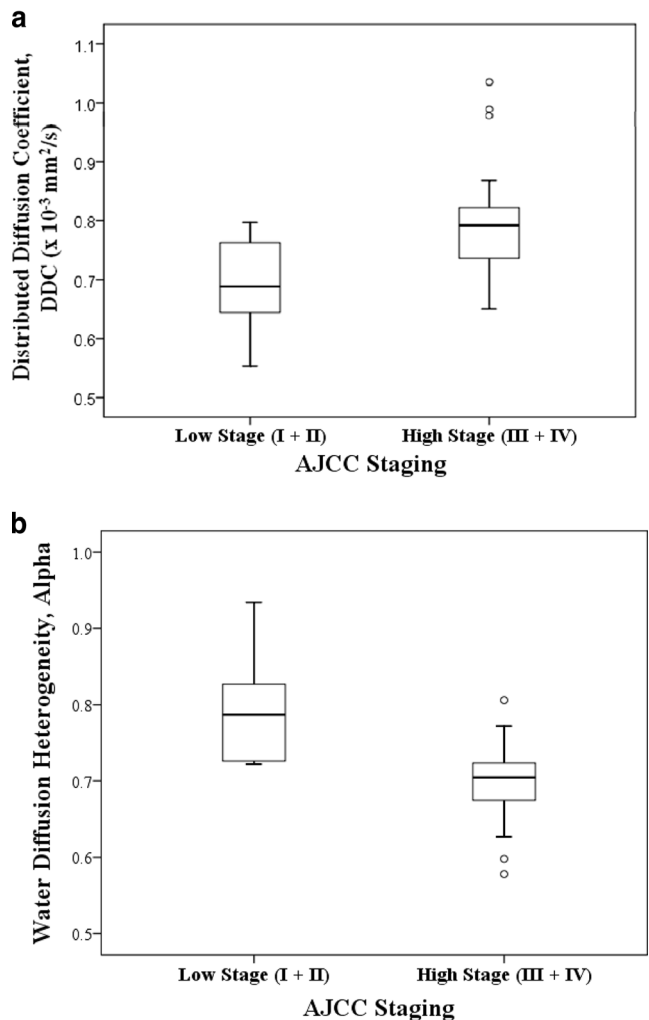


Fig. 2 Box plots showing distribution of **a** distributed diffusion coefficient (DDC) water and **b** diffusion heterogeneity (α) between low and high AJCC stages

Table 3 Optimal cut-off values under 95 % confidence intervals for AJCC staging according to ROC curve analysis with respective sensitivity, specificity, positive likelihood ratio and negative likelihood ratio

	Cut-off value	Sensitivity (%) (95 % CI)	Specificity (%) (95 % CI)	Pos LR (95 % CI)	Neg LR (95 % CI)
AJCC stage					
DDC	$0.692 \times 10^{-3} \text{ mm}^2/\text{s}$	94.4 (81.3–99.3)	64.3 (35.1–87.2)	2.64 (1.3–5.4)	0.09 (0.02–0.4)
α	0.720	72.2 (54.8–85.8)	100 (76.8–100)	–	0.28 (0.2–0.5)

AJCC American Joint Committee on Cancer, CI confidence interval, Pos LR positive likelihood ratio, Neg LR negative likelihood ratio

stage group ($p < 0.001$). On the basis of the ROC curve analysis (Fig. 3), their optimal cut-off values (with respective sensitivity, specificity, positive likelihood ratio, negative likelihood ratio and area under curve) were DDC = $0.692 \times 10^{-3} \text{ mm}^2/\text{s}$ (94.4 %, 64.3 %, 2.64, 0.09, 0.833); $\alpha = 0.720$ (72.2 %, 100 %, –, 0.28, 0.911). Stepwise regression analysis revealed that both the DDC ($p < 0.001$) and α ($p < 0.001$) were reliable independent predictors. On the basis of the area under curve (AUC), α was the more powerful parameter, though no statistical significance could be reached on direct comparison between DDC and α ($p = 0.125$).

Discussion

DW MR imaging has received much attraction in the evaluation and characterisation of tumour behaviours with regard to its water diffusivity, showing promising results, in particular with various different types of head and neck tumours especially NPC. Different diffusion models had been devised to better account for the complicated non-Gaussian diffusion behaviour of biological tissues, as well as providing additional

information on different aspects of tissue properties [12–14]. IVIM diffusion MR imaging had been shown to be useful in the functional assessment and characterisation of NPC, providing one with the pure diffusion and perfusion properties. The stretched exponential diffusion model is an alternate method that can provide us with the tissue heterogeneity and diffusion simultaneously. It was found to be more reliable and reproducible than the monoexponential and biexponential models [11] and was shown to be successful in tissue characterisation in brain and prostate tumours [11, 15]. In particular, Kwee et al. [15] found that high grade glioma had a significantly lower α value than that of the normal brain structure, suggesting its usefulness in the assessment of histological heterogeneity and hence potential grading of tumours. This type of diffusion model, however, has received little attention in head and neck tumours and has not been properly assessed in NPC so far.

Our results showed that the stretched exponential diffusion model with utilization of higher b values was feasible in the evaluation of NPC. It was also advantageous in that it provided with us the new parameter α , reflecting the tissue heterogeneity, which characterised deviation of the signal attenuation from monoexponential form. α was found to be statistically significantly lower in the high stage group of NPC when compared to the low stage group of NPC. This signifies considerable tumoral or histological heterogeneity in high stage tumours, which is likely related to a higher degree of cellular pleomorphism, presence of intravoxel microscopic necrotic foci, and intravoxel heterogeneity in vascular structures [15]. On the contrary, DDC was found to be statistically significantly higher in the high stage group of NPC and negatively correlated with α . This is in concordance with past studies showing an inverse correlation between tumour cellularity and tumour diffusion coefficient [15, 16]. Nevertheless, this inverse relationship warrants further larger cohort study for confirmation. Histopathological correlation would also be helpful in understanding their relationship. α was a more reliable independent predictor and with a cut-off value of 0.72 it was able to differentiate between low and high stage groups (sensitivity 72.2 %, specificity 100 %).

One major limitation of this study was the lack of histopathological correlation with the heterogeneity index in both the low and high stage groups of NPC. Inclusion of other

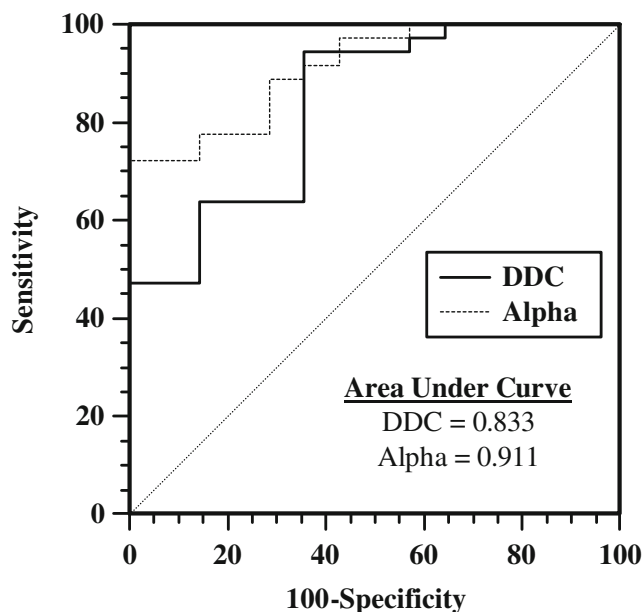


Fig. 3 ROC curves analysis for DDC and α with respective areas under curves in AJCC staging

histological subtypes of NPC would be of great interest to test for the ability of the heterogeneity index in their differentiation. Data reproducibility is another major concern [17]. The use of the very high b values required in this stretched exponential diffusion model could lead to impaired SNR. The highest b value (2,500 s/mm²) chosen in our study was based on the adequate and satisfactorily obtained SNR above background noise in the region of the nasopharynx. Because of the poor SNR, NPC with small tumour volume had to be excluded because of inadequate SNR within the small fraction of voxel. In the present study, the evaluation of reproducibility was limited to repeated measurements within one single acquisition only. Further study focusing on the reproducibility from different acquisitions within the short term should be carried out to establish its clinical utility as a quantitative tool. A larger cohort study would be helpful to further consolidate our preliminary findings. Despite these drawbacks, our promising results have shed light on this stretched exponential diffusion model as a potential new method in the evaluation of NPC. In addition, it can also potentially help in treatment monitoring and in post-treatment assessment by studying serial changes in both DDC and α .

In conclusion, the stretched exponential diffusion model is feasible and useful in the noninvasive tissue characterisation of NPC. The heterogeneity index α is robust and can potentially help in staging and grading prediction.

Acknowledgments The scientific guarantor of this publication is Prof. Khong Pek Lan. The authors of this manuscript declare relationships with the following companies: Dr. Q Chan is currently employed by Philips Medical Systems. This study has received funding by University Grants Council (UGC) seed funding from The University of Hong Kong, project no. 201112159010.

No complex statistical methods were necessary for this paper. Institutional review board approval was obtained. Written informed consent was obtained from all subjects (patients) in this study. Approval from the institutional animal care committee was not required because this study did not involve animals. Study subjects or cohorts have not been previously reported.

Methodology: prospective, diagnostic or prognostic study, performed at one institution.

References

- Lai V, Khong PL (2014) Updates on MR imaging and ¹⁸F-FDG PET/CT imaging in nasopharyngeal carcinoma. *Oral Oncol* 50:539–548
- Lai V, Li X, Lee VHF, Lam KO, Chan Q, Khong PL (2013) Intravoxel incoherent motion MR imaging: comparison of diffusion and perfusion characteristics between nasopharyngeal carcinoma and post-chemoradiation fibrosis. *Eur Radiol* 23:2793–2801
- Lai V, Li X, Lee VHF et al (2014) Nasopharyngeal carcinoma: comparison of diffusion and perfusion characteristics between different tumour stages using intravoxel incoherent motion MR imaging. *Eur Radiol* 24:176–183
- Hauser T, Essig M, Jensen A et al (2013) Characterization and therapy monitoring of head and neck carcinomas using diffusion-imaging-base intravoxel incoherent motion parameters – preliminary results. *Neuroradiology* 55:527–536
- Le Bihan D, Breton E, Lallemand D, Aubin ML, Vignaud J, Laval-Jeantet M (1988) Separation of diffusion and perfusion in intravoxel incoherent motion MR imaging. *Radiology* 168:497–505
- Riches SF, Hawtin K, Charles-Edwards EM, de Souza NM (2009) Diffusion-weighted imaging of the prostate and rectal wall: comparison of biexponential and monoexponential modeled diffusion and associated perfusion coefficients. *NMR Biomed* 22:318–325
- Bennett KM, Schmainda KM, Bennett RT, Rowe DB, Lu H, Hyde JS (2003) Characterization of continuously distributed cortical water diffusion rates with a stretched-exponential model. *Magn Reson Med* 50:727–734
- Bennett KM, Hyde JS, Rand SD et al (2004) Intravoxel distribution of DWI decay rates reveals C6 glioma invasion in rat brain. *Magn Reson Med* 52:994–1004
- Bennett KM, Hyde JS, Schmainda KM (2006) Water diffusion heterogeneity index in the human brain is insensitive to the orientation of applied magnetic field gradients. *Magn Reson Med* 56:235–239
- Hall MG, Barrick TR (2008) From diffusion-weighted MRI to anomalous diffusion imaging. *Magn Reson Med* 59:447–455
- Mazaheri Y, Afaq A, Rowe DB, Lu Y, Shukla-Dave A, Grover J (2012) Diffusion-weighted magnetic resonance imaging of the prostate: improved robustness with stretched exponential modeling. *J Comput Assist Tomogr* 36:695–703
- Lu Y, Jansen JF, Mazaheri Y, Stambuk HE, Koutcher JA, Shukla-Dave A (2012) Extension of the intravoxel incoherent motion model to non-gaussian diffusion in head and neck cancer. *J Magn Reson Imaging* 36:1088–1096
- Jansen JF, Stambuk HE, Koutcher JA, Shukla-Dave A (2010) Non-gaussian analysis of diffusion-weighted MR imaging in head and neck squamous cell carcinoma: a feasibility study. *AJNR Am J Neuroradiol* 31:741–748
- Vandecaveye V, De Keyzer F, Dirix P, Lambrecht M, Nuyts S, Hermans R (2010) Applications of diffusion-weighted magnetic resonance imaging in head and neck squamous cell carcinoma. *Neuroradiology* 52:773–784
- Kwee T, Galban CJ, Tsien C et al (2010) Intravoxel water diffusion heterogeneity imaging of human high-grade gliomas. *NMR Biomed* 23:179–187
- Provenzale JM, Mukundan S, Barboriak DP (2006) Diffusion-weighted and perfusion MR imaging for brain tumor characterization and assessment of treatment response. *Radiology* 239:632–649
- Braithwaite AC, Dale BM, Boll DT, Merkle EM (2009) Short- and midterm reproducibility of apparent diffusion coefficient measurements at 3.0-T diffusion-weighted imaging of the abdomen. *Radiology* 250:459–465